IOP PUBLISHING JOURNAL OF PHYSICS B: ATOMIC, MOLECULAR AND OPTICAL PHYSICS

J. Phys. B: At. Mol. Opt. Phys. **41** (2008) 192001 (15pp) doi:10.1088/0953-4075/41/19/192001

TOPICAL REVIEW

Atomic processes in antihydrogen experiments: a theoretical and computational perspective

F Robicheaux

Department of Physics, Auburn University, AL 36849-5311, USA

Received 17 June 2008
Published 10 September 2008
Online at stacks.iop.org/JPhysB/41/192001

Abstract

One possible route for a precision test of the CPT theorem is to perform spectroscopic measurements on the antihydrogen atom and compare the results with those from hydrogen. We present a review of the existing theoretical and computational treatments of atomic processes important for understanding the experiments to make and trap the antihydrogen atom. The emphasis of this review is on the behaviour and properties of the charged species in these devices (electrons, positrons and antiprotons) and the properties of the antihydrogen that can be formed.

1. Introduction

Making and trapping antihydrogen ($\bar{H}$) atoms might appear to be a relatively simple procedure: cold charged particles naturally become neutral atoms if given the chance and countless groups routinely trap neutral atoms using a variety of methods. Unfortunately, the simplest methods that convert charged particles to neutral atoms (collisions with solids or neutral atoms/molecules) would not work for $\bar{H}$ because the antimatter version of solids or atoms or molecules is not readily available. This means that relatively inefficient processes must be employed to make the $\bar{H}$. Also, the typical energy scale for the constituent particles, the positron (e^+) and the antiproton ($\bar{p}$), is set by voltages in the trap which give energies five orders of magnitude larger than the largest energy for which the neutral can be trapped. Because the $\bar{H}$ will hit the wall of the trap in a time less than 1 ms after it forms, the $\bar{H}$ needs to be formed from cold positrons and, especially, cold $\bar{p}$'s. This restriction means that the charged particles need to be handled carefully.

The purpose of this review is to describe the main physics processes that are or could be important for understanding the formation and properties of $\bar{H}$. The focus will be on the atomic processes. Plasma processes also play a very important role in these experiments. Unfortunately, an adequate review of the charged species' large-scale motion and their collective properties would double the length of this review. This review will mainly address theoretical and computational issues since there is a recent review [1] of this area from an experimental perspective.

The basic configuration of the $\bar{H}$ experiments is that of a nested Penning trap suggested two decades ago [2]. This can be thought of as a long tube constructed from short, cylindrical electrodes. The electrodes can be raised to their individual voltages so that the positrons are attracted to regions of negative (or low) voltage and the antiprotons, $\bar{p}$, are attracted to the positive (or high) voltage. A large magnetic field is along the trap axis and prevents charged particles from moving radially outward. To make the $\bar{H}$ atoms, it is necessary to have the $\bar{p}$'s go through a region of relatively dense positrons (or vice versa). This can be accomplished through many different schemes (some are addressed below). The rough size of the trap is a couple centimetres in radius and 0.5–1 m in length. But, under typical operation, the charged particles extend only over a small radial region and only over a length measured in centimetres along the trap.

Once the $\bar{H}$ is formed it needs to be trapped. The current attempts at trapping will use a spatially varying magnetic field as in typical atom trapping set-ups (for details of the ALPHA apparatus, see [3]). The magnetic moment of the ground state of $\bar{H}$ is essentially the same as the magnetic moment of a free positron (or electron) and gives a well depth of roughly

2/3 K per T change in magnetic field. The magnetic minimum is constructed by adding mirror coils separated by a distance of roughly 1/4 m and adding a cylindrical multipole field by having high currents run back and forth across the outside of the trap. With the uniform B-field along the trap axis, these spatially varying magnetic fields give a minimum in the magnitude of the B-field halfway between the mirror coils and near the radial centre of the trap. Considering the difficulty in constructing these coils a magnetic field depth of roughly 1 T is a reasonable starting point for calculations. See [4–6] for recent experimental advances.

Aspects of all processes described in this review have been theoretically or computationally investigated from the 1960s back to the 1920s. However, the $\bar{\mathrm{H}}$ experiments are for a range of parameters that have not been treated until quite recently. The novelty arises due to the combination of low temperature and high magnetic fields that are present in these experiments. Almost all of the processes are qualitatively changed from those occurring at high temperatures or low magnetic fields. Also, the direction of the change is not always the same. For some processes, the magnetic fields enhance the rates while for others the magnetic fields strongly suppress certain processes.

The reader will probably note that the majority of the theory and the calculations use classical mechanics to obtain results. Since the positron is light and has low energy, the reader might be concerned about the reliability of the results to be presented. Unfortunately, most of the processes cannot be calculated within a quantum framework and, thus, the simplest argument, good agreement between quantum and classical calculations, is not available. The best that can be done is to note the situations where classical and quantum results tend to strongly differ and compare to the systems described here. (1) Quantum and classical results differ strongly when the classical process is forbidden but can occur quantum mechanically. An example is when a positron passes by a $\bar{\mathrm{H}}$; when the impact parameter is too large, the positron cannot exchange enough energy with the atom to change the principle quantum number even if enough energy is available, whereas the quantum process is nonzero for any finite impact parameter due to the exchange of virtual photons. (2) Quantum and classical results differ strongly when the classical result is allowed but through a small opening in phase space. An example is an electron going through a small hole; quantum mechanically the transmission through a small hole can be exponentially suppressed when the transverse size of the hole is smaller than 1/2 of the wavelength. (3) Quantum and classical results differ strongly when interference is important. An example is when the transition is going from a particular initial state i to a particular final state f. (4) Quantum and classical results differ strongly when diffraction of the waves is important; this is a special case of (1). For example, quantum electrons impinging on a sphere will have a nonzero probability for being found directly behind the sphere but classical electrons have zero probability. (5) Quantum and classical results differ strongly when small quantum numbers are involved.

For the processes discussed below, none of these situations *seems* to occur. Since some of the processes are for chaotic systems and many coupled degrees of freedom, it is not always obvious that a given system can be treated classically. As an example that will be discussed below, consider three-body recombination where there is the collision between two positrons in the field of a $\bar{\mathrm{p}}$. In this case, the process is classically allowed (so (1) does not apply), the recombination is into states with a size of $\sim$1 μm whereas the wavelength is $\sim$70 nm (so (2) does not apply), the recombination is into a huge number of states with differing quantum numbers (so (3) does not apply), the phase space structures do not vary much over a wavelength (so (4) does not apply) and the states that are populated by recombination have quantum numbers $\sim$100 (so (5) does not apply).

This review is organized as follows. Section 2 treats various processes that are related to the temperature of the charged particles and of the resulting $\bar{\mathrm{H}}$; this section includes the cooling from cyclotron radiation, the collisional coupling between the motion along the field and the cyclotron radiation, the cooling of the $\bar{\mathrm{p}}$ from collision with positrons, the cooling of the $\bar{\mathrm{H}}$ due to random emission of photons and the heating of the $\bar{\mathrm{p}}$ and $\bar{\mathrm{H}}$ due to collisions. Section 3 describes the changes to the $\bar{\mathrm{H}}$ in a strong magnetic field; this section includes the description of a guiding centre atom and more deeply bound atoms. Section 4 describes to the processes that can be used to form the $\bar{\mathrm{H}}$; this section includes radiative recombination, stimulated radiative recombination, charge transfer, three-body recombination, a description of the types of states formed and the radiative cascade process which determines how quickly the $\bar{\mathrm{H}}$ reaches the ground state. Section 5 discusses different possibilities for trapping the $\bar{\mathrm{H}}$ atoms; this section includes references to trapping based on spatially varying magnetic fields, trapping due to the polarizability of the atom, and trapping in combined magnetic and electric multipole fields. Section 6 describes the few calculations that attempted to simulate all aspects of the $\bar{\mathrm{H}}$ experiments.

2. Temperature

One of the key ingredients in the success of cooling and trapping $\bar{\mathrm{H}}$ will depend on getting the charged particles to temperatures of a few kelvin. The rates for making $\bar{\mathrm{H}}$ increase with decreasing temperature. Also, the fraction of $\bar{\mathrm{H}}$ that can be trapped increases with decreasing temperature because the trapping depth of the ground state will be approximately 1/2–2/3 K.

2.1. Cooling

The only true cooling mechanism in the $\bar{\mathrm{H}}$ experiments is from the emission of photons from the circular motion of the positrons and/or electrons in the strong magnetic field. All other types of motion are cooled only to the extent that they can couple to the cyclotron motion of the light species. The radiative decay rate of the cyclotron motion can be computed either quantum mechanically or using the simple radiation from a classically oscillating dipole [7]. They give the same decay rate

$$\Gamma_{\mathrm{cyc}} = \frac{4e^4B^2}{12\pi\varepsilon_0 m_e^3 c^3} = 0.39B^2\ \mathrm{Hz\ T^{-2}}, \qquad (1)$$

where the dependence on the square of the magnetic field is clear. The radiative decay rate for a $\bar{p}$ is smaller by a factor of $(m_e/m_p)^3 \sim 2 \times 10^{-10}$ and is thus negligible.

There are several important features of equation (1) that should be noted. First, this rate causes the cyclotron motion to come into thermal equilibrium with the radiation field at frequencies near the cyclotron frequency. Thus, if the electrons or positrons start at a higher temperature than the radiation field, they will cool to that temperature. Conversely, if the electrons or positrons through a mechanical manipulation start at a lower temperature, then they will increase in temperature. Second, the cyclotron radius, mv/eB, of the electrons or positrons is typically 100 nm or less so the magnetic field is very nearly constant across the orbit. This means that only photons resonant with the cyclotron motion, $f_{\rm cyc} = eB/(2\pi m_e)$, will be absorbed and emitted and, thus, only those photons participate in the cooling or heating of the cyclotron motion. Also, this decay rate assumes the photons are emitted into vacuum. If a resonant chamber were to (partially) enclose the positrons or electrons, then the density of photon states at the cyclotron frequency could be enhanced which could lead to much faster equilibration times.

2.2. *Collision cooling*

From the previous section, the only degrees of freedom that cool on a reasonable time scale is the cyclotron motion. The other degrees of freedom only cool to the extent that energy can be transferred from them to the cyclotron motion. Since the cyclotron motion of the positrons and electrons has the highest frequency in this system, the most efficient way to couple to the cyclotron motion is through collision. Estimating the collision rate from the field-free rates can give orders of magnitude errors.

In [8], it was shown that the cyclotron motion of two electrons during an electron–electron collision was an adiabatic invariant. This means that the amount of energy transfer from the motion along the B-field into the cyclotron motion is exponentially suppressed when the electrons are far enough apart so that the collision time, $b/v_\parallel$ (impact parameter over parallel velocity), is long compared to the cyclotron period $2\pi m_e/(eB)$. At low energies, there is another constraint in that the electrons cannot approach to a distance closer than $d_{\rm min} = {\rm e}^2/\left(\pi\epsilon_0 m_e v_\parallel^2\right)$ which sets the scale for the minimum impact parameter. Thus, only to the extent that $2\pi m_e v_\parallel/(eB) > d_{\rm min}$ is it possible to transfer energy from the motion parallel to the magnetic field to the cyclotron motion which can radiate away the excess energy. This expression can be rearranged to give a minimum parallel kinetic energy of $(1/4)m_e v_\parallel^2 \sim (1/4)\left[{\rm e}^3 B/\left(2\pi^2\varepsilon m_e^{1/2}\right)\right]$ that can couple to the cyclotron motion.

The actual evaluation of the collision rate is somewhat complicated by the fact that it is the rare high-velocity collisions that give the coupling between parallel and perpendicular motion. However, it is still instructive to make simple estimates for the experimental parameters. As an example, using the parameters from the ATHENA experiment [9], the magnetic field was approximately 3 T which gives a minimum parallel kinetic energy of 32 K; using the parameters from the ATRAP experiment [10], the magnetic field was approximately 5.4 T which gives a minimum parallel kinetic energy of 47 K. This simple estimate shows that it is not at all obvious that the parallel temperatures of the positrons and electrons were as low as that for the cyclotron motion.

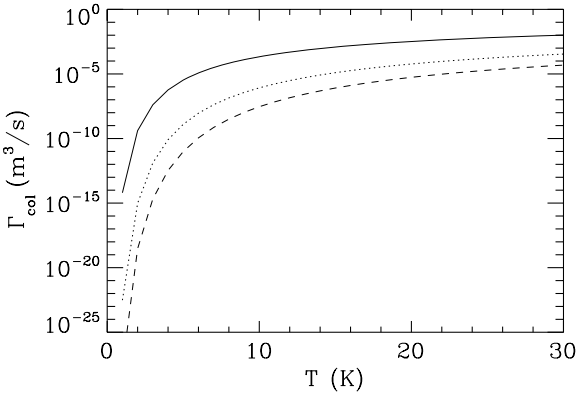

Figure 1. The collision rate, $\Gamma_{\rm col}$, for coupling the parallel and perpendicular motions in a strong magnetic field: the solid line is for 1 T, the dotted line is for 3 T and the dashed line is for 5 T.

The ideas of [8] were revisited in [11–13]. In [8], an expression for the rate that energy scatters from the parallel to the perpendicular motion is given as

$$\Gamma_{\rm col} = n\bar{v}\bar{b}^2 I(\bar{\kappa}), \tag{2}$$

where n is the density, $\bar{v} = \sqrt{2k_B T_\parallel/m_e}$ is the parallel thermal velocity, $\bar{b} = 2e^2/(4\pi\epsilon k_B T_\parallel)$ is proportional to the distance of closest approach and $\bar{\kappa} = eB\bar{b}/(m\bar{v})$ is proportional to the ratio of collision time and the cyclotron period. The function I was given a more accurate expression [13] as

$$I(x) \simeq \exp\left[-\frac{5(3\pi x)^{2/5}}{6}\right] \times \left[\frac{1.83}{x^{7/15}} + \frac{20.9}{x^{11/15}} + \frac{0.347}{x^{13/15}} + \frac{87.8}{x^{15/15}} + \frac{6.68}{x^{17/15}}\right]. \tag{3}$$

In figure 1, the collision rate is shown for magnetic fields of 1, 3 and 5 T. It is clear that at lower temperatures and/or high magnetic fields the collision rate could be substantially slower than the radiation rate.

To see how the collisions affect the cooling of the parallel motion, we solved for the coupled rate equation that included radiation damping for $T_\perp$ and collisions coupling $T_\parallel$ and $T_\perp$. When simulations are performed at a density of 2×10^8 cm^{-3}, the background radiation temperature of 15 K and 3 T magnetic field (roughly ATHENA parameters), the cooling was solely determined by the cyclotron radiation rate; the collision rate was much higher than the radiation rate for these parameters. When simulations are performed at a density of 4×10^7 cm^{-3}, the background radiation temperature of 4.2 K and 5.4 T magnetic field (roughly ATRAP parameters), the $T_\parallel$ and $T_\perp$ become decoupled because the collision rate is so low. The evolution of the two temperatures are shown in figure 2 when they are both started at 30 K. This result indicates that the parallel temperature of the light species might

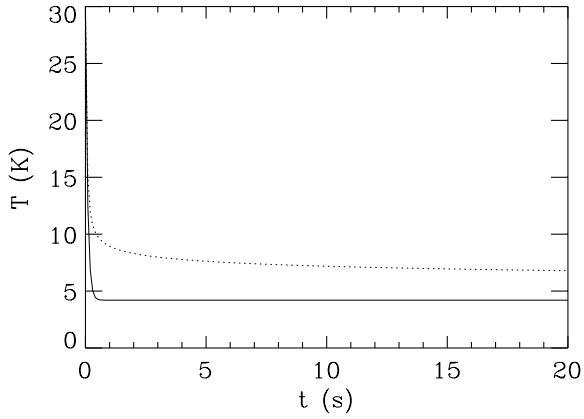

Figure 2. The results of a simulation of the parallel (dotted line) and perpendicular (solid line) temperature as a function of time when both start at 30 K. The simulation includes coupling of the cyclotron motion to the radiation field and coupling between parallel and perpendicular motion including the suppression due to strong magnetic field. The magnetic field strength was taken to be 5.4 T and the density was 4×10^7 cm^{-3}.

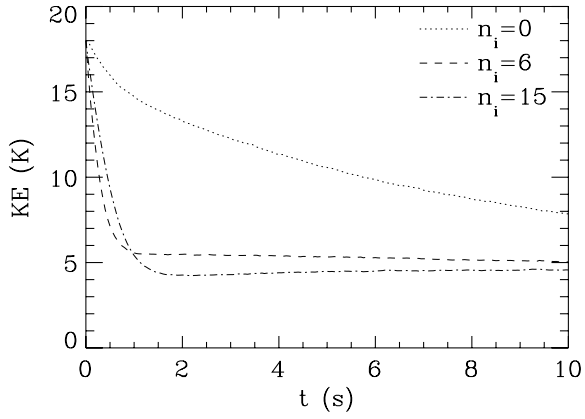

Figure 3. The average kinetic energy at $z = 0$ for an electron distribution that initially has $KE = 18$ K. The dotted line is when all of the electrons start with $n = 0$, the dashed line is for $n = 6$ and the dash-dot line is for $n = 15$; n is the number of quanta in the cyclotron motion. The only processes included in the calculation is the motion of the electron along a spatially varying magnetic field and the fluctuating magnetic dipole moment due to emission and absorption of photons. There is no electrostatic potential to provide a restoring force. From figure 1 of [14].

be substantially higher than the perpendicular temperature if very low temperatures are sought in high magnetic fields.

There have been proposals to use ultralow energy electrons to cool the $\bar{p}$'s to temperatures below 1 K. The assumption that the $\bar{p}$'s will reach the temperature of the electrons is dubious at such a low temperature and high magnetic fields. For this reason, the results of these simulations will not be reviewed.

2.3. *Fluctuation cooling*

The weak coupling between parallel and perpendicular motion at low temperatures and high magnetic fields could cause the parallel temperature of the plasma to be substantially higher than desired. In [14], the possibility of cooling the parallel motion by directly coupling to the radiation field was considered. It was noted the parallel motion will couple to the radiation field through the fluctuation in the magnetic moment if the electrons or positrons are in a spatially varying magnetic field. Figure 3 shows the amount of cooling in the parallel temperature when the electron or positron has different initial quanta in the cyclotron motion. This shows it is possible to cool the parallel motion without collisions. However, the effect is largest for magnetic fields with the largest spatial variation. For the likely experimental parameters, it seems that the effect will not be significant.

2.4. *$\bar{p}$ cooling*

There are two aspects that need to be considered for the cooling of $\bar{p}$'s. There is the initial cooling of the $\bar{p}$'s due to their interaction with an electron plasma. During this stage, the $\bar{p}$'s are cooled from energies of order keV down to energies of order several K (1 meV $\simeq$ 12 K). During this stage, they are confined to a small fraction of the total trap length.

For any mixing process where positrons are mixed into a $\bar{p}$ plasma, the cooling by electrons is important. Typically, the density and number of electrons can be very high so that the $\bar{p}$'s come into thermal equilibrium with the electrons on reasonable experimental times. If necessary, the electrons can be removed by kicking them with an electric field pulse. A technique [16] was proposed for cooling $\bar{p}$'s below the thermal temperature of the trap. This technique uses the negative ion of Os to sympathetically cool the $\bar{p}$'s. The idea is to hold the $\bar{p}$'s in a region that also contains a substantial population of Os^-. The Os^- is laser cooled and collisions with the $\bar{p}$'s will cool them. The $\bar{p}$'s will need to start somewhat cold so they do not detach the electron from the negative ion and spiral into the nucleus. The constraint on the starting temperature of the $\bar{p}$'s is not great, probably anything less than 1000 K will be fine.

The other aspect that needs to be considered is the cooling of $\bar{p}$'s that are launched into a positron plasma [10, 15]. For this process it is hoped that the $\bar{p}$'s are already somewhat cold. The cooling of $\bar{p}$'s in the positron plasma is a vital process because the rate of this process determines whether the $\bar{H}$'s are formed before or after the $\bar{p}$'s come into thermal equilibrium with the positrons.

The dominant cooling mechanism is coupling to plasma waves when the $\bar{p}$'s have a high velocity compared to the thermal velocity of the light species. As long as the velocity of the $\bar{p}$ is larger than the thermal velocity of the electrons or positrons, the slowing can be computed as due to a linear response of the medium [17]. Nersisyan *et al* [18] give an expression for the stopping power

$$S = -\frac{dE}{dl} \tag{4}$$

as a three-dimensional integral, see their equation (8). The functions $F(s)$ and $G(s)$ can be simplified to expressions involving exponentials or to standard Dawson integrals.

These expressions for $\bar{p}$ slowing have been used in simulations of $\bar{H}$ experiments, but the results of calculations

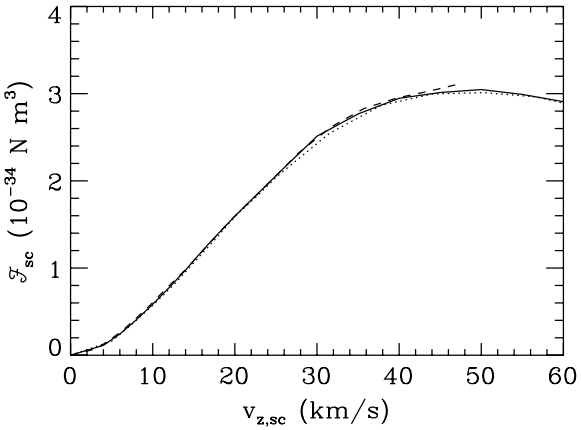

Figure 4. The force per unit density, $\mathcal{F}_{sc}$ exerted on a $\bar{p}$ from a beam of positrons at the perpendicular temperature of 4 K and at a scaled velocity parallel to the field, $v_{z,sc}$, but in different magnetic fields. There are three different magnetic fields: 1 T (solid line), 1/2 T (dotted line) and 2 T (dashed line). The results have been scaled so that $v_{z,sc} = v_z/(B/T)^{1/3}$ and $\mathcal{F}_{sc} = \mathcal{F}(B/T)^{2/3}$. From figure 5 of [22].

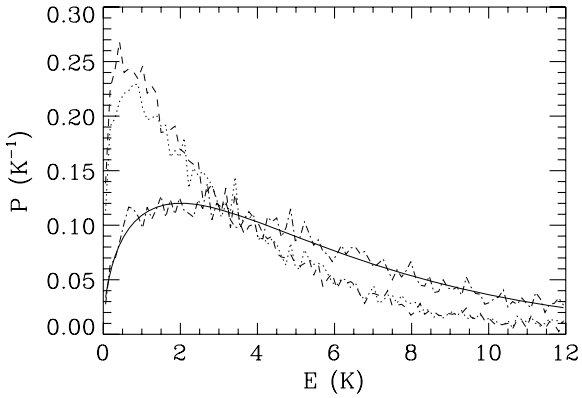

Figure 5. The energy distribution, P, of atoms after they have reached $n = 1$. The atoms start with $n = 25$ and in a thermal distribution with a temperature of 4 K. The dashed line is for atoms starting in a circular state while the dotted line is for atoms in a random distribution of $m \geqslant 15$. The dot-dashed line shows the initial distribution and the solid line is the thermal distribution: $\propto \sqrt{E}\exp(-E/k_BT)$. Substantial cooling occurs due to the time-dependent change of the magnetic moment with the circular states showing a slightly stronger effect. From figure 4 of [23].

relying on this treatment of $\bar{p}$ slowing are suspect. The reason is that only a small fraction of the $\bar{H}$'s form when the $\bar{p}$'s have a speed greater than the thermal velocity of the positron. Thus, the competition between $\bar{H}$ formation and $\bar{p}$ slowing cannot be predicted with any accuracy in the crucial span of time when $\bar{H}$ is being formed.

One of the common features of all calculations is that the cyclotron motion of the $\bar{p}$ interacts more strongly with the positron plasma than the motion along the field. The reason is that the perpendicular component of the impulse delivered to a $\bar{p}$ as a single positron passes tends to a finite value whereas the parallel component is approximately 0. For the perpendicular motion, a perturbative treatment of the collision is sufficient to understand the thermalization of the perpendicular motion of the $\bar{p}$. In general, the expressions for the thermalization rate (for example, see [19–21]) are quite complicated and so will not be reproduced here. For our purposes, it is sufficient to know that the thermalization rate of the $\bar{p}$'s cyclotron motion is much higher than that of the parallel motion.

As a first step in addressing the lack of understanding when the parallel component of the $\bar{p}$ velocity is less than the positron thermal velocity, Hurt *et al* [22] performed calculations of the individual collisions between positrons and $\bar{p}$'s. The calculation emphasized the coupling of the $\bar{p}$'s velocity along the field to the positron plasma. Figure 4 shows a plot of the average force exerted on a stationary $\bar{p}$ from a beam of positrons as a function of the speed of the positrons. Because the classical system can be scaled, the results from three different magnetic fields can be collapsed to one curve. When a thermal average is performed over positron velocities, Hurt *et al* [22] found that the drag force on a $\bar{p}$ with speed less than the thermal speed of the positrons could be written as

$$F_{\text{drag}} = -m_p V_z n \frac{4.3 \times 10^{-12}}{B} \text{ T m}^3 \text{ s}^{-1}, \qquad (5)$$

where m_p is the proton mass, V_z is the z-component of the $\bar{p}$'s velocity, n is the positron number density and B is the magnetic field strength. This expression was accurate to within 10% for $|V_z| < 10$ km s^{-1}, positron temperatures between 4 and 32 K and magnetic fields between 1/2 and 2 T. The coupling to plasma waves is *not* included in this expression so the actual drag force will be greater than this by an amount not known at this time.

Finally, there is another drag whose strength is unknown. As the $\bar{p}$ travels through the positron plasma, positrons can be temporarily captured into very weak states with binding energies less than k_BT. If a positron is weakly attached, then the motion of the $\bar{p}$ will be affected as it emerges from the edge of the plasma. In general, it will lose a small amount of energy when the positron is stripped away. The amount of energy lost by the $\bar{p}$ will increase with the binding energy of the positron. It will also depend on the curvature of the electric potential near the edge of the positron plasma.

2.5. $\bar{H}$ cooling

Two theoretical papers [23, 24] suggested the remarkable result that $\bar{H}$ might substantially cool after it is formed due to radiative decay of microwave photons. This process can occur because the magnetic moment of the atom changes (usually decreases) when the photon is emitted. Figure 5 shows the resulting energy distribution of ground state $\bar{H}$ atoms if the initial $\bar{H}$ started in a state with principal quantum number 25 with a 4 K thermal distribution. It is clear that the final energy distribution has substantially shifted to lower energy. For atoms with an initial 4 K distribution, roughly three times more atoms could be trapped than without this effect.

In general, a Monte Carlo simulation with the trap parameters would be needed to obtain an accurate assessment of the size of this effect. However, the physics of this situation is amenable to a simple but effective approximation based on the fact that the radiative lifetimes increase rapidly with

principal quantum number. This means that for high principal quantum number the photons are emitted at random times but the $\bar{H}$ typically move a substantial distance between emissions. This gives a series of random emissions over the whole of the trap. At low principal quantum numbers, the photon emissions are so closely spaced in time that the $\bar{H}$ is essentially fixed in space. This gives a large change in magnetic moment from one random position in the trap. For typical trap dimensions, the principal quantum numbers around 15 gives the division between slow and rapid photon emission. As an example, see figure 2 of [23].

Cesar *et al* [25] considered the possibility for enhancing this cooling through the use of microwaves. The basic idea is that a relatively weak microwave (field strengths of mV cm^{-1}) can strongly couple to the *electric* dipole moment of the atom and cause the angular momentum to precess without changing the principal quantum number. This precession can be made to occur at larger magnetic field where the $\bar{H}$ is travelling slowly. Thus, the $\bar{H}$ will not gain as much kinetic energy when it travels to the magnetic minimum. Also, lower angular momentum states radiate faster than the high angular momentum states. For a single, fixed microwave frequency and strength, enhancements of the trapping fraction up to 50% were calculated.

2.6. $\bar{p}$ heating

In [26], the $\bar{p}$ mixing with the positron plasma was stimulated by heating the $\bar{p}$'s with a 825 kHz RF field. The number of $\bar{p}$'s in the experiment varies over time from a high of 2×10^5 down to a much smaller number as the $\bar{H}$ is formed and/or $\bar{p}$'s are lost. The expected velocity of the $\bar{p}$'s when they reach the positron plasma is not given. However, in [27], the measured velocity of the $\bar{H}$'s was reported to be comparable to a kinetic energy of 200 meV which is roughly 2300 K. A later modelling [28] of extra processes in the ATRAP experiment noted that the measurements could be consistent with temperatures in the range of 1–10 meV (12–120 K).

From the information given in [26], it is not possible to fully model the heating of the $\bar{p}$'s to give estimates of their thermal properties. From the paper, there is a 1 V peak-to-peak drive field on one of the electrodes for 10 s. The depth of the well that the $\bar{p}$'s are being driven over is roughly 10 V. The $\bar{p}$'s gain energy as a collective plasma from the RF field. Collisions between $\bar{p}$'s will cause the energy to go into heat in both the parallel motion and the cyclotron motion.

For this situation, the $\bar{p}$'s heat by the collision between pairs. The energy of the $\bar{p}$'s along the magnetic field must be extremely high compared to the K scale hoped for. As a way of estimating the various heating rates, one can use the usual scattering between point particles but with the magnetic field cutting off scattering for impact parameters larger than $\sim v_{\|} m_p/(eB)$. Taking $v_{\|} = 3 \times 10^4$ m s^{-1} (corresponds to approximately 4.7 eV), this maximum distance is approximately 58 μm in a 5.4 T field. If 2×10^5 $\bar{p}$'s are uniformly spread over a radial region of 1 cm, then each $\bar{p}$ can interact with approximately six others. As an estimate of the heating rate of the cyclotron motion, the standard heating rate

$$\frac{1}{\tau} = n_p v \frac{e^4 \ln \Lambda}{4\pi \varepsilon_0^2 m_p^2 v^4} \tag{6}$$

can be used where the Coulomb logarithmic divergence is cutoff by the magnetic field to give $\Lambda = (4\pi\varepsilon_0 m_p v^2/e^2)(m_p v/eB)$; τ is approximately the $1/e$ time for energy to transfer between parallel and perpendicular motion. Estimating the $\bar{p}$'s density by assuming they are in a cylinder of radius 1 cm and length 3 cm gives $n_p \sim 2 \times 10^{10}$ m^{-3}. Using the parameters in this paragraph gives $\tau \sim 400$ s. Because the parallel energy scale is of order 10 eV, this must mean that the cyclotron motion is roughly gaining 25 meV per second. The RF field is on for a time that is roughly 10 s, thus it seems that a temperature scale of 100 meV is reasonable for this experimental arrangement.

2.7. $\bar{H}$ heating

Pohl *et al* [28] raises an important issue about the possible heating of $\bar{H}$ once they are formed. Suppose that an $\bar{H}$ is formed in a Rydberg state and is trapped by the spatially varying magnetic field. It is still in the region where the charged particles are moving. There are two collision processes that are available for causing the $\bar{H}$ to heat and be lost from the trap.

If the $\bar{H}$ passes through the positron plasma, a charge exchange process can occur. After the charge exchange, the $\bar{H}$ could be in a high-field-seeking state that will be attracted to the walls of the trap instead of being repelled. The charge exchange will be somewhat larger than the geometrical size of the $\bar{H}$. The maximum radial size of the atom is $r_{\max} \simeq 2a_0\nu^2$, where $a_0 = 0.529 \times 10^{-10}$ m is the Bohr radius. Thus, to within an order of magnitude,

$$\Gamma_{ce} \sim 4n\sqrt{k_B T/m_e}(2a_0\nu^2)^2, \tag{7}$$

where n is the positron density, T is the temperature of the positron plasma and ν is the principal quantum number of the $\bar{H}$ atom. Taking 4 K for the temperature, the charge exchange rate is $\Gamma_{ce} \sim n\nu^4 3 \times 10^{-16}$ m^3 s^{-1}. Typical densities of these experiments is $10^{13} - 10^{15}$ m^{-3}. Taking a density of 10^{14} m^{-3} gives a charge exchange rate of $\Gamma_{ce} \sim \nu^4 0.03$ s^{-1}. As will be discussed below, the radiative decay rate decreases rapidly with principal quantum number. Thus, the $\bar{H}$ will either be in the ground state when it passes through the positron plasma or in states with $\nu > 20$. It is clear that charge exchange will not be important for the ground state. However, the charge exchange rate is high even for $\nu = 20$. To get a gauge of the importance of charge exchange, the distance that the $\bar{H}$ can travel in the plasma before an exchange takes place, v/Γ_{ce}, is a useful quantity. Taking the $\bar{H}$ speed to be 100 m s^{-1} means there is a charge exchange for every 2 cm it moves through a positron plasma at $\nu = 20$, while it is 4 mm for $\nu = 30$. Since most of the $\bar{H}$ is formed in even higher quantum states, this could be a significant effect. The amount of charge transfer is reduced by the fact that the $\bar{H}$ only spends a fraction of its time in the positron plasma; unfortunately, the $\bar{H}$'s are created in the positron plasma and tend to return to that region more

often than other regions of the trap which will raise the number of charge transfers over that from simple estimates from the fraction of the trap occupied by the plasma.

The other heating process also comes from charge exchange, but with the $\bar{p}$'s not the positrons. This was the process discussed in [28]. Typically, the $\bar{p}$'s will have several electron volts of energy. The only differences in the estimates from above is that a 5 eV $\bar{p}$ has a speed of approximately 30 km s^{-1} as opposed to 10 km s^{-1} of a 4 K positron and the $\bar{p}$ density is often substantially less than that for positrons. In the ATHENA experiments, the $\bar{p}$ number was roughly 1% of those in a typical ATRAP experiment. Thus, ATRAP was much more likely to experience problems with this heating effect. Using the $\bar{p}$ density from the previous section, a rough estimate of the charge exchange rate is $\Gamma_{ce} \sim \nu^4 10^{-4}$ s^{-1}. Thus, this charge exchange to $\bar{p}$'s seems like it will be much smaller than that from the positron plasma unless the $\bar{p}$ density is significantly raised. However, this is partly an illusion because the $\bar{p}$'s cover a much larger region of the trap and thus the charge transfer can happen during a larger fraction of the $\bar{H}$'s lifetime. For the ATHENA experiments, the number of positrons was several orders of magnitude larger than the number of $\bar{p}$'s, and thus it is clear that charge transfer to $\bar{p}$'s will be negligible. For the ATRAP type parameters, the number of $\bar{p}$'s was comparable to that for positrons and the two types of charge transfer may occur with similar effective rates.

3. $\bar{H}$ in a strong magnetic field

Even a magnetic field of 1 T can strongly modify the properties of the $\bar{H}$ from that in zero field. For simplicity, we can consider three different degrees of binding. For very deeply bound atoms, the magnetic field only perturbatively affects the motion and the main change is a paramagnetic energy shift and a diamagnetic interaction that mixes the ℓ states for a given principal quantum number, ν, and angular momentum projection m; the energy eigenstates can be obtained by diagonalizing the diamagnetic term within a fixed ν manifold and has been treated by many authors, e.g., see [29]. For very weakly bound atoms, the size of the cyclotron orbit of the positron is much smaller than the size of the atom so that the motion decouples into a cyclotron motion for the positron, a bounce motion in the z-direction from the attractive $1/r$ potential, and a circular motion of the centre of the cyclotron orbit due to the $\vec{E} \times \vec{B}$ drift. These are often called guiding centre atoms. Finally, there is an intermediate regime between these where the motion is likely to be chaotic.

The guiding centre atoms have many special properties. Before delving into the full blown dynamics, it is useful to consider the motion of the positron when the $\bar{p}$ is held fixed and the positron has a trajectory where the distance to the $\bar{p}$, R, is much larger than the cyclotron radius *and* the amplitude of motion along the field is small compared to R. To a good approximation, the motion can be thought of as three nearly uncoupled motions. (1) The cyclotron motion with an angular frequency of eB/m_e. (2) The z-bounce motion with a frequency $\omega = (e/R^{3/2})/\sqrt{4\pi\varepsilon_0 m_e}$ which can be found by expanding the Coulomb potential to second order in z: $V = -e^2/(4\pi\varepsilon_0 R) + (1/2)m_e(e^2/[4\pi\varepsilon_0 m_e R^3])z^2$. (3) The $\vec{E} \times \vec{B}$ drift velocity causes the positron to circle the $\bar{p}$ with an angular frequency of $v/R = (E/B)/R = e/(4\pi\varepsilon_0 R^3 B)$.

The motions (1) and (3) lead to opposite signs of the magnetic dipole moment. The cyclotron motion gives a negative dipole moment with a size of KE/B; thus, this motion causes the atom to be attracted to low fields. The $\vec{E} \times \vec{B}$ motion gives a positive dipole moment with a size of $|PE|/B$; thus, this motion causes the atom to be attracted to high fields. Choi *et al* [30] used this competition to trap Rb atoms in Rydberg states; in this experiment, the binding energy was much less than the kinetic energy in the cyclotron motion so that the atoms were trapped in the spatially varying magnetic fields. But it is important to note the opposite regime. When the binding energy of the guiding centre atom is greater than the energy in the cyclotron motion, the atom will be a high-field seeker, i.e. attracted to the walls of the trap. Note that guiding centre atoms from three-body recombination will tend to be of this type and, therefore, not amenable to trapping.

The simple treatment above does not hint at some of the interesting features of guiding centre atoms. Kuzman *et al* [31] and Vrinceanu *et al* [32] investigated some of the basic properties of these atoms. One of the conserved quantities is the pseudomomentum [33]:

$$\vec{K} = M\frac{\mathrm{d}\vec{R}}{\mathrm{d}t} - e\vec{r} \times \vec{B}, \tag{8}$$

where $\vec{R}$ is the centre-of-mass position and $\vec{r}$ is the vector that points from the $\bar{p}$ to the positron; one can show $\vec{K}$ is conserved simply by taking the derivative of it with respect to t and substituting the forces for the second derivatives. When the atom moves perpendicular to the field, the pseudomomentum can be large enough so that the $\bar{H}$ can form stable bound states with very large dipole moments. Vrinceanu *et al* [32] also investigated how the large magnetic field can affect the strength of the electric field needed to strip the positron from the atom. The very large dipole moments (both electric and magnetic) will affect the centre-of-mass motion of the $\bar{H}$ through spatially varying electric and magnetic fields [34, 35]. If the centre-of-mass kinetic energy of the atoms is low enough, it is even possible that these atoms could be trapped at the edge of the positron plasma.

Finally, Dubin [36] noted that it may be possible to form guiding centre positive ions, i.e. one $\bar{p}$ and two positrons. These ions had one relatively deeply bound positron and another that was more weakly bound. Although the formation of such ions is probably rare, there have been examples seen in the molecular dynamics studies of [37, 38].

4. $\bar{H}$ formation

Now we turn to the processes that can be used to form $\bar{H}$. In all processes, the positron and $\bar{p}$ need a third body present to combine into bound $\bar{H}$. Three completely different types of particles have been suggested in the role of the third body: photons (radiative recombination), electrons (charge transfer) and positrons (three-body recombination). Each of the processes has different strengths and weaknesses, but the

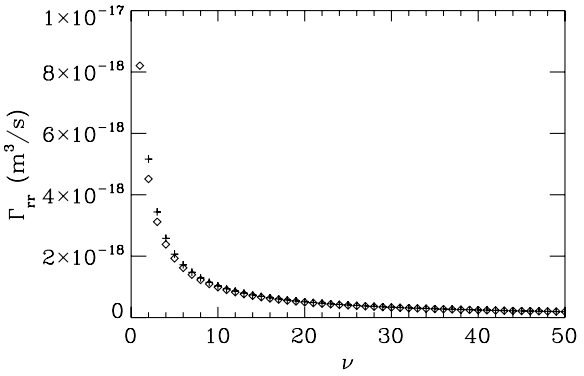

Figure 6. The radiative recombination, Γ_{rr}, rate into all of the states in each degenerate manifold for a 4 K thermal distribution: numerical solution of the quantum expression (diamond) and approximate solution from Kramers cross section (+). The total radiative recombination rate at 4 K is 4.3×10^{-17} m^3 s^{-1}.

one that appears to be the most promising is that of three-body recombination. The strong magnetic fields and low temperatures modify the rates and sometimes the qualitative results from each process.

4.1. Radiative recombination

When there is no magnetic field present, the computation of the radiative recombination rate is an old, solved problem in quantum mechanics. The radiative recombination cross section (in atomic units) from a positron with energy E into a state with principal quantum number ν and angular momentum ℓ, m is given by

$$\sigma_{rr} = \frac{\pi}{2E}(E - E_{\nu,\ell})^3 \sum_{\ell m\prime,i} \frac{8\pi}{3c^3} \left|\left\langle \psi_{\nu\ell m}|r_i|\psi^{(c)}_{E\ell\prime m\prime}\right\rangle\right|^2, \qquad (9)$$

where r_i are the three dipole operators $r_0 = z$ and $r_\pm = \mp(x \pm \mathrm{i}y)/\sqrt{2}$, the bound states are normalized in space and the continuum states have energy normalization $\left\langle \psi^{(c)}_{E\ell m}\middle|\psi^{(c)}_{E'\ell' m'}\right\rangle = \delta(E - E')\delta_{\ell\ell'}\delta_{mm'}$. With current computational resources, it is relatively simple to compute the rate for any parameters needed instead of storing a fitting formula, but, for completeness, the Kramers approximation to the radiative recombination cross section into all states within the manifold of degenerate states is

$$\sigma_{K,rr} = 2.1 \times 10^{-22} \frac{E_0^2}{\nu E(E_0 + \nu^2 E)} \text{ cm}^2, \qquad (10)$$

where $E_0 = 13.6$ eV and E is the incoming energy of the positron. To obtain the radiative recombination rate, multiply the cross section by the speed of the positron and average over a thermal distribution. Figure 6 shows the branching ratio for the $\bar{\mathrm{H}}$ to recombine into a state with principal quantum number ν summed over all angular momenta ℓ, m. One of the features that is initially surprising is that the $\bar{\mathrm{H}}$ most probably forms in the deepest bound states; this is in contrast to classical radiative recombination which preferentially populates the weakest bound states.

At 4 K, the radiative recombination rate into states with principal quantum numbers less than 50 is 4.3×10^{-17} m^3 s^{-1}. Taking the positron density to be 10^{14} m^{-3}, gives a recombination rate of 4.3×10^{-3} s^{-1}. If a $\bar{\mathrm{p}}$ spends one-third of the time in the positron plasma, then 10^4 $\bar{\mathrm{p}}$'s will give a $\bar{\mathrm{H}}$ formation rate of 15 Hz. If all of these were trappable $\bar{\mathrm{H}}$'s, then the rate would be low but within the range of what can be detected. However, the fraction of the atoms that could be trapped is not encouraging. First, only half of the atoms will have the correct sign of magnetic moment that can be trapped. Next, only the atoms with kinetic energy less than the trap depth can be trapped. For a 4 K distribution with a trap depth of 2/3 K, the number of trapped atoms is approximately 5%. Thus, approximately 1/40 of the $\bar{\mathrm{H}}$ formed could be trapped giving a rate of roughly 1/3 Hz. This is probably too low to detect.

The magnetic field substantially changes the rates of various processes so it is worthwhile investigating how the magnetic field affects the radiative recombination rate. Radiative recombination is the inverse of photoionization and can be obtained from it by detailed balance. As a first attempt at understanding the effect of magnetic fields on radiative recombination, it is useful to qualitatively treat photoionization in a strong magnetic field. The first experiments on photoionization in a strong magnetic field were reported in [39]. The photoionization cross section was modified from the field-free value by an energy dependence that oscillated on a scale proportional to $\hbar\omega_{\mathrm{cyc}} = \hbar eB/m_e$; this is the separation of the thresholds for ionization leaving the electron with different quanta in the cyclotron motion. Also, the states that are most strongly populated from radiative recombination are themselves only perturbatively changed from the field-free states. Thus, one should expect very little change in the radiative recombination rate if $\hbar eB/m_e < k_B T$ because the modulation in the energy-dependent cross section will be washed out by the spread of energies of the positron. In the ATHENA experiment, $B = 3$ T which gives $\hbar eB/(m_e k_B) = 4.0$ K compared to their temperature of 15 K; thus, the field-free recombination rates will be accurate. In the ATRAP experiment, $B = 5.4$ T which gives $\hbar eB/(m_e k_B) = 7.2$ K compared to their temperature of 4.2 K; thus, the radiative recombination rate might be considerably modified. Finally, in the next generation of experiments, the $\bar{\mathrm{H}}$ will likely be formed in a lower magnetic field, 1 T, to increase the magnetic trap depth; at this field, $\hbar eB/(m_e k_B) = 1.3$ K compared to the likely temperature of 4.2 K which means field-free rates will give accurate estimates of the actual rate.

The one case where the radiative recombination rate was possibly modified by the magnetic field was the ATRAP experiments at 5.4 T and 4.2 K. Horndl *et al* [40] gave a classical treatment of the problem by computing the change in the classical phase space in a region near the nucleus. They found an increase in the rate for C^{6+} radiative recombination due to chaotic scattering increasing the number of times the electron passes near the nucleus. It may seem intractable to consider performing a fully quantum calculation, but the problem can be reformulated in a manner that allows a relatively simple quantum calculation. Suppose the quantum energy levels are computed for a spherical region, radius R, centred on the nucleus where the wavefunction is forced to go to 0 at $r = R$. This will give both positive and negative energy

states with the positive energy states discretized because of the boundary condition at $r = R$. One can now define a quantity

$$\Gamma_{rr}(R) = \frac{4\pi R^3}{3} \sum_j \gamma_j(R) \exp(-E_j/k_B T)/ \sum_j \exp(-E_j/k_B T) \quad (11)$$

where the sums are performed over all states with $E_j > 0$ and γ_j is the radiative decay rate from state j to states deeply bound enough to survive the electric fields in the trap. In the limit that $R \to \infty$, this definition yields the usual radiative recombination rate. Fortunately, this quantity converges at reasonable values of R which allow calculations to occur. In calculations for 4 K positrons, I find that the radiative recombination rate hardly changes for magnetic field strengths up to $\sim$ 4 T. At 5 T, the rate has increased by 10% and it has increased by approximately 20% at 6 T. It is interesting that almost all of the change is for recombination into states with principal quantum number larger than 35. Unlike three-body recombination, the radiative decay rates are not strongly affected by the magnetic field. Perhaps insight into this process can be gained from the calculations of [41] who found that the collision of a positron with a $\bar{p}$ in a strong magnetic field can lead to temporarily bound states at positive energies. The radiative recombination from these resonance states will be greatly increased over that when the positron passes the $\bar{p}$ only once.

The radiative recombination rate can be enhanced if the photon emission is stimulated by the presence of additional photons. This was seen experimentally in weak magnetic fields [42, 43]. CO_2 lasers have strong output at frequencies that could take a threshold electron to states with principal quantum number near $n = 10$. Enhancement by factors over 1000 were obtained. They give an expression for the gain in the recombination into a manifold of degenerate states as

$$g = \frac{I\lambda^3}{h\delta\nu 8\pi c}, \quad (12)$$

where I is the laser power, λ is the wavelength, h is Planck's constant, $\delta\nu$ is the 'frequency spread of the photon beam' and c is the speed of light. This expression is not very useful for the $\bar{p}$ experiments because the positrons are not in a beam. If the photoionization rate out of the bound state is smaller than the radiative decay to lower states, the stimulated recombination rate is

$$\Gamma_{rr,\mathrm{stim}} = \frac{1}{2}\left(\frac{m_e}{2\pi k_B T}\right)^{3/2} \frac{7.5\times 10^{-6} n I \lambda^3 E_0 a_0^2}{\nu m_e^2 c}, \quad (13)$$

where n is the positron density, a_0 is the Bohr radius, $E_0 = 13.6\,\mathrm{eV} = 2.18\times 10^{-18}$ J, ν is the principal quantum number, λ is the wavelength, I is the intensity of the light and c is the speed of light; the fraction $1/2$ is a crude approximation to account for the laser polarization. This expression assumes the photons have an energy uncertainty much less than the thermal energy and that the laser is tuned to an energy much closer to threshold than $k_B T$. Amoretti *et al* [44] attempted to measure the increase in recombination by using a 10.96 μm laser with 100 W cm^{-2} of power. They estimated they could enhance the rate from 24 s^{-1} to 84 s^{-1} but did not see an increase in the total number. Using the equation above gives an enhancement of $\sim$200 s^{-1} instead of 60 s^{-1}. However, the simple estimate from above needs to be reduced because the laser power gives a re-ionization rate comparable to the radiative decay rate. There have been more detailed treatments of the theory (e.g. [45]).

Wesdorp *et al* [46] introduced a different variation for stimulating recombination through time-varying fields. In these papers, the authors showed that an electric field kick while an electron passed an ion could cause the electron to recombine with the ion. In the $\bar{H}$ experiments, the strength and duration of the kick are somewhat limited. From figure 3 of [46], it is apparent that the atoms that are made can be stripped by the electric fields in the $\bar{H}$ traps which limits the usefulness of this technique.

4.2. Charge transfer

In [47], an ingenious technique was suggested for the formation of $\bar{H}$ based on a two-step process. In the first step, a Rydberg atom is passed through a positron plasma where a charge transfer takes place to give positronium in a Rydberg state. The positronium is now free to cross field lines and can move to a region where $\bar{p}$'s are trapped. A second charge transfer can take place giving the formation of a Rydberg $\bar{H}$. Since each charge transfer tends to roughly preserve the binding energy, the $\bar{H}$ has a binding energy comparable to that of the original Rydberg atom. Thus, the starting state of the $\bar{H}$ can be controlled to some extent. The calculations demonstrating the effect were performed with $B = 0$ in order to obtain results in a reasonable time.

This process was seen in [48, 49] where Cs was the atom used as the starting point. Because the experiments were performed in a strong magnetic field which might affect the dynamics, Wall *et al* [50] performed the calculations in magnetic fields of 1, 2 and 4 T for initial principal quantum numbers of 30, 40 and 50. They found that the initial charge transfer rate was roughly geometrical

$$\langle v\sigma\rangle \simeq 5.2(2\nu^2 a_0)^2\sqrt{k_B T/m_e}, \quad (14)$$

where a_0 is the Bohr radius, ν is the principal quantum number, and T is the temperature of the positron plasma. The accuracy is at least 25% for $30 \leqslant \nu \leqslant 50, 4\mathrm{K} \leqslant T \leqslant 8K$ and $1\mathrm{T} \leqslant B \leqslant 4\mathrm{T}$. The Rydberg positronium does not emerge purely isotropically but can be suppressed in the direction of the magnetic field. Figure 7 shows the distribution of principal quantum number for the $\bar{H}$ formed after the second charge transfer; the $\bar{H}$ tends to have energies peaked just below the initial binding energy of the Rydberg atom and with a tail to more deeply bound states. Somewhat surprisingly, the distribution of magnetic moments after the second charge transfer leads to a suppression of trappable atoms from what would be expected from a statistical distribution. This is not a good news since it reduces the number of usable $\bar{H}$. The reason for the asymmetry will be discussed below.

Lu *et al* [51] computed the charge transfer from Rydberg positronium to a $\bar{p}$ in a strong magnetic field. This is the second

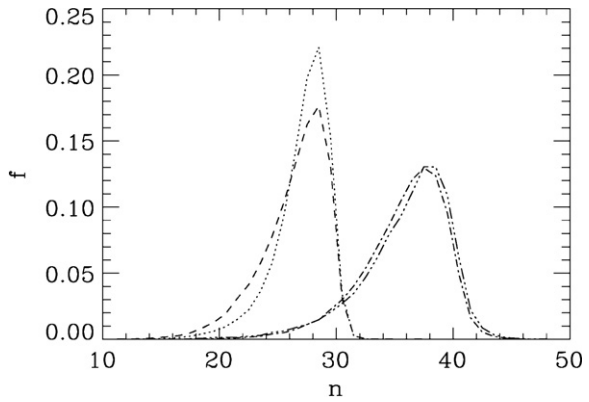

Figure 7. The fraction, f, of $\bar{H}$ formed with energies corresponding to principal quantum number n from a double charge exchange: excited atom plus positron goes to ion plus highly excited positronium then highly excited positronium plus $\bar{p}$ goes to highly excited $\bar{H}$ plus electron. The dotted line is for $B = 1$ T and the Rydberg atom initially in $n = 30$, the dashed line is for $B = 4$ T, $n = 30$, the dash-dot line is for $B = 1$ T, $n = 40$ and the dash-dot-dot-dot line is for $B = 4$ T, $n = 40$. The magnetic field does not strongly affect the binding energy of the atoms. The peak is slightly shifted down in n from that of the initial atom. From figure 2 of [50].

stage of the process discussed in the previous paragraph. As in the treatment above, they solved the time-dependent classical motion using a Monte Carlo technique to generate different trajectories. They found a substantial reduction in the charge transfer cross section from that with no magnetic field, but of a size that would not negate the effectiveness of this process.

There have also been a large number of quantum calculations for charge transfer during positronium collisions with $\bar{p}$'s. These calculations have sometimes included the effect of a laser field on the cross section. The calculations are for ground state or near ground state positronium. As a rough rule, the size of the cross section is roughly the geometrical size of the positronium (or the laser excited virtual state). For the ground state, a positronium flux of roughly 10^{15} s^{-1} through an area of 1 cm^2 would be needed to get a transfer rate of approximately 1 Hz. As an example, see [52] and the references therein.

Although the multiple steps involved will probably reduce the overall rate of formation, this avenue will likely be pursued because the $\bar{p}$ can be held in place and be cold. Since almost all of the kinetic energy of the $\bar{H}$ comes from the original kinetic energy of the $\bar{p}$, a method that starts from cold $\bar{p}$ has distinct advantages. However, using this method to make trappable $\bar{H}$ is not straightforward. The method is useless unless the $\bar{p}$ are cold which likely means the $\bar{p}$ are part of an electron-$\bar{p}$ plasma or the electrons have been removed in a process that leaves the $\bar{p}$'s cold. The latter method has never been demonstrated. The first method has its own problems because the electrons can collide with the $\bar{H}$ and destroy it through a third charge exchange. To determine the overall probability for forming trappable $\bar{H}$, one would also need to compute the probability it can escape the electron-$\bar{p}$ plasma. Under apparently reasonable configurations, the survival probability can be less than 1% and depends strongly on the density and shape of the plasma and the ratio of electrons to $\bar{p}$'s.

4.3. Three-body recombination

The most favourable process leading to $\bar{H}$ seems to be three-body recombination. The initial capture step occurs when two positrons collide in the vicinity of a $\bar{p}$ so that one loses enough energy to become bound while the other gains energy. If the resulting $\bar{H}$ is in a plasma, then further collisions can either reionize the atom or drive it to more deeply bound states. In the $\bar{H}$ experiments, the positron plasmas are from 1 mm to a few centimetres thick. This means the $\bar{H}$ is in the plasma for a short amount of time; thus, the time development of the distribution of binding energies are particularly important. Several papers report on calculations of recombination at very low temperatures and claim to give insight into recombination for the $\bar{H}$ experiments. Unless the calculations include the effect of strong magnetic fields, they will not be reviewed here.

Glinsky and O'Neil [53] introduced the first treatment of the three-body recombination in a strong magnetic field. In this calculation, the positrons were constrained to move on straight lines which can be thought of as the $B \to \infty$ limit. For steady state recombination, they expressed the rate in the commonly used form

$$\Gamma_{\mathrm{TBR}} = Cn^2 v b^5, \tag{15}$$

where n is the positron density, $v = \sqrt{k_B T/m_e}$ and $b = e^2/(4\pi\varepsilon_0 k_B T)$. This expression can be thought of as the velocity of the positron, v, times the cross section, b^2, times the probability for finding another positron within that volume, nb^3. They found that $C = 0.070 \pm 0.01$ which is an order of magnitude less than the $B = 0$ rate. They also provided data on the time dependence of the bound state distribution. The bound state distribution of the $\bar{H}$ was measured in [26]. The time-dependent calculations were used in [54] to argue that this energy distribution matched that of the experiments, but [55] argued that the parameters of the experiment were quite different from those assumed in [54] so that the agreement was not good.

Robicheaux and Hanson [56] performed the next calculations of the three-body recombination in a strong magnetic field. First, the calculation of [53] was repeated using a completely different method giving a more precise value $C = 0.072 \pm 0.002$. Then the next order term in the guiding centre approximation was included which is the $\vec{E} \times \vec{B}$ drift. Including this effect increased the rate by changing C to 0.11 ± 0.01 where the ± 0.01 was due to a weak variation with temperature and magnetic field; table I of [56] gave values of C for different B and T. This is roughly a 60% increase from the $B \to \infty$ limit. This paper also pointed out the fact that a moving $\bar{p}$ will recombine as long as its velocity is less than the thermal velocity of the positrons; the recombination rate has only dropped by a factor of 2 when the $\bar{p}$ speed is one-third of the thermal speed. For a 4 K positron plasma, this corresponds to a kinetic energy of 140 meV (1600 K) for the resulting $\bar{H}$. This means it is important that slowing of the $\bar{p}$ occurs quickly,

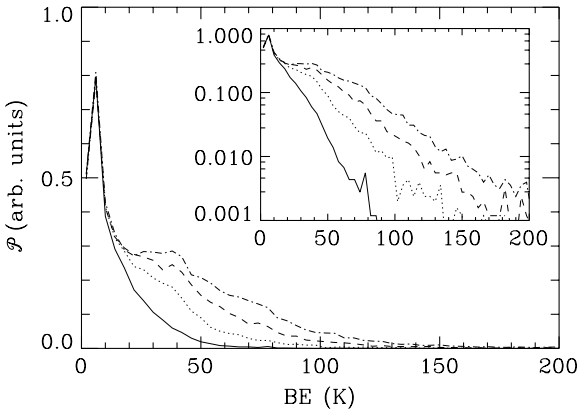

Figure 8. The energy distribution, $\mathcal{P}$, of $\bar{H}$ as a function of binding energy for different times in the positron plasma. The solid line is at 20 μs, the dotted line is at 40 μs, the dashed line is at 60 μs and the dash-dot line is at 80 μs. The inset is the same data but on a log-scale for the y-axis. For this calculation, the temperature is 4 K, the magnetic field is 1 T and the density is 1.37×10^7 cm^{-3}. Adapted from figure 4(a) of [58].

otherwise very few of the $\bar{H}$ will be low enough in energy to be trapped.

Robicheaux [57] repeated the calculations for three-body recombination but now solving for the full classical motion of the positrons. At 1 T, the total recombination rate agreed with the guiding centre approximation only at 4 K. The coefficient C varied from 0.11 at 4 K, to 0.15 at 8 K and to 0.19 at 16 K. This is because the size of the cyclotron orbit is becoming comparable to or larger than the size of the atom as the temperature increases; note that the size of the atom decreases like T^{-1}, while the radius of the cyclotron orbit increases like $T^{1/2}$. This calculation was also able to obtain distributions for the magnetic moment; the importance of this result will be discussed below. To give an example of the time dependence, figure 8 shows the time dependence of the binding energy for a positron plasma at 4 K, in a 1 T magnetic field and a density of 1.37×10^7 cm^{-3}. Note that the distribution of binding energy less than 10 K does not change with time. The more deeply bound states evolve over the time scale shown. It is important to note that a $\bar{H}$ travelling at 100 m s^{-1} will cross 1 cm of plasma in 100 μs. Thus, time scales longer than those shown are not extremely important. If the density increases, the overall number of recombined atoms increase and the population at deeper binding evolves faster.

Pohl *et al* [28] provided an important insight into the three-body recombination in a strong magnetic field. From a full three-dimensional calculation for the positrons, they found that there are much more deeply bound atoms than an extrapolation from weakly bound states (e.g. the region shown in their figure 8) would suggest. They found this extra population resulted from a single collision between a weakly bound $\bar{H}$ and a free positron that gave a large change in energy. This population is not seen in calculations based on the guiding centre approximation and was attributed to the chaotic motion of a positron in a Coulomb plus magnetic field. The size of the effect will be less for fields of 1 T compared to 5.4 T in the ATRAP experiments.

Robicheaux [58] addressed the issue of three-body recombination when both electrons and positrons are present. This situation might occur if positrons are mixed into a $\bar{p}$ plasma. Typically, the $\bar{p}$ plasma is cooled by the presence of electrons and, therefore, the question arises whether all of the electrons need to be removed before attempting recombination. When electrons are present, they can contribute in a positive way to the recombination by causing positrons to lose energy in the field of the $\bar{p}$. However, they can also decrease the recombination by either scattering the positron to higher energy states or by charge transfer which destroys the $\bar{H}$. Simple relations for how the presence of electrons affect the recombination were presented. The most important result was that the electrons qualitatively decrease the recombination rate even when the density of positrons was four times that of the electrons.

Before leaving the issue of three-body recombination, note that there is another possibility that has not been addressed in either calculations or experiment. This is the possibility that a two-stage process can be used. In the first stage, electrons are mixed with a positron plasma. In a three-body recombination step, Rydberg positronium can be formed. The positronium can then cross field lines to where a cold $\bar{p}$ plasma is held. At this point, a charge transfer can take place which would give a cold $\bar{H}$. This is a variation of the scheme in [47–50]. However, no one has computed the three-body recombination rate when only light species are present and it is not even clear whether the process can occur in a small plasma.

Fedichev [59] gave estimates for the rate that the binding energy of weakly bound atoms lose energy in a positron plasma due to the far collisions with the plasma positrons. However, it was pointed out in [60] that the increasing frequency of rotation with increasing binding energy negates that treatment. Bass and Dubin [60] give a collision rate in terms of a double integral over a K_1 Bessel function which should give a more accurate treatment of the time dependence of the binding energy.

Hu *et al* [37] and Vrinceanu *et al* [38] performed molecular dynamics simulations of thousands of $\bar{p}$'s in a positron plasma (several thousand in the MD simulation). They followed the trajectories using a special symplectic propagator and were able to follow the particles for up to 500 ns. Unfortunately, this length of time is only sufficient to see the original positron collision capture step so that none of the $\bar{H}$ atoms would survive the electric fields in the actual traps; the important time scale for the $\bar{H}$ formation that can survive the electric fields of the trap is roughly 100 times longer, see figure 8.

4.3.1. Three-body recombination reconsidered. Because the $\bar{p}$'s quickly cross the positron plasma, the three-body recombination only has a passing resemblance to the steady state process. In essence, a bare $\bar{p}$ is introduced to the plasma, a distribution of positrons around it relaxes into very weakly bound states, and then, maybe, a lucky collision drives a positron into a relatively deeply bound level that can survive the trap fields. Instead of the usual scaling of three-body recombination, perhaps the arrested nature of the recombination will give a different scaling.

Since the $\bar{H}$'s need to survive the trap fields, they need to recombine into states with maximum extent R where the electric field from the $\bar{p}$ is roughly that from the trap fields, i.e. $F_{\text{trap}} \sim e/(4\pi\varepsilon_0 R^2)$. A possible argument for different scaling would be: the recombination rate into a state that can survive the fields of the trap is proportional to the probability of finding a positron within a distance R of the $\bar{p}$ ($n[4\pi R^3/3]$), times the cross section for a collision that could remove enough energy so that it becomes bound (πb^2), times the flux of positrons nv. Since R does not scale with temperature, $b \propto 1/T$, and $v \propto \sqrt{T}$, the rate will scale like $n^2 T^{-3/2}$. This is not nearly as fast a decrease with temperature as the steady state rate, $n^2 T^{-9/2}$.

4.4. Types of states formed

The strong magnetic field affects the types of states that are formed in various processes that generate $\bar{H}$. In all of the processes discussed above, the direction of the angular momentum would be randomly oriented. Also, the magnitude of the angular momentum at a given binding energy would be strongly mixed in the case of collisions or have an easily calculable form for radiative recombination. The magnetic field defines a direction in space. Because the magnetic field is strong, it could easily be the case that the angular momentum will be oriented with respect to the field. This is important because it is the direction of the magnetic moment relative to the magnetic field which will determine whether the $\bar{H}$ has any possibility of being trapped.

Because radiative recombination mostly populates the most deeply bound states (see figure 6), the states formed will only be weakly changed from the distribution in zero magnetic field. Thus, radiative recombination will equally populate the m-levels for a given ν, ℓ to a good approximation. The stimulated recombination will also be that for zero magnetic field and thus will more strongly depend on the polarization of the laser field.

For the double charge transfer [47–50], the magnetic field can strongly change the orientation of the magnetic moment. Figure 9 shows the average value of $m(xv_y - yv_x)$ which is proportional to the magnetic moment of the atom but is *not* the canonical angular momentum. The distribution is clearly skewed to positive values which means more high-field seekers are formed than low-field seekers. Part of the hope in using this method for giving $\bar{H}$ was that the magnetic moment would be large in magnitude and give low-field-seeking atoms. It is precisely this type of atom which is suppressed in figure 9.

For three-body recombination, the type of state that is formed depends on the binding energy of the state. It was already noted that [28] found an extra population $\bar{H}$ for deeply bound states. This is clearly good news in the sense that deeply bound atoms are less likely to be destroyed by other processes in the trap. However, the effect is not as important at 1 T, e.g. see figure 8 which shows a simple power-law dependence down to binding energies of 200 K which corresponds to principal quantum number $\nu = 28$. Robicheaux [57] examined the important question of how

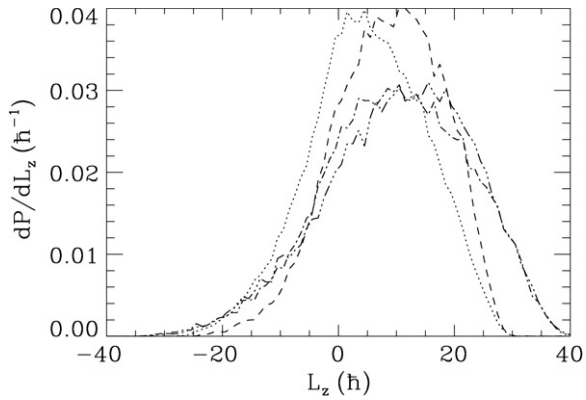

Figure 9. The distribution, dP/dL_z, of $\bar{H}$ formed with the positron having time average angular momentum, $L_z = m\langle(xv_y - yv_x)\rangle$, along the B-field; although the magnetic moment is proportional to the time average of L_z, the quantity $xv_y - yv_x$ is not a constant of motion. The lines are for the same cases as in figure 7. Unlike the $B = 0$ case, the L_z is not centred at 0. The implications are discussed in the text. From figure 3 of [50].

the magnetic moment depends on the temperature of the plasma and the binding energy of the $\bar{H}$. The calculations were performed in a 1 T plasma at temperatures of 4, 8 and 16 K. The main finding was that the formation of $\bar{H}$'s attracted to low magnetic fields was suppressed compared to those attracted to high fields, i.e. the walls of the trap. There was a weak dependence on temperature with the higher temperature tending to give a larger fraction of $\bar{H}$ attracted to low fields. Also, the more deeply bound the $\bar{H}$ the more likely it would be attracted to low fields. However, the fraction of atoms with large magnetic moments (greater than 10 K T^{-1}) and attracted to low fields was less than 8% for all of the cases examined.

4.5. Radiative cascade

An important aspect of the $\bar{H}$ formation is how quickly it can reach the ground state. Supposing an excited $\bar{H}$ is formed and trapped, it will spend most of the time travelling through the trap in a strong magnetic field. The question naturally arises about the time needed to radiate away the internal energy and reach the ground state. In zero magnetic field, the low angular momentum states have lifetimes that increase as the cube of the principal quantum number while the highest angular momentum states have lifetimes that increase as the principal quantum number to the fifth power.

Guest *et al* [61] computed the radiative decay rates for very highly excited states. These are the states that correspond to the classical guiding centre atoms discussed above [31, 32]. They were able to separate the decay into radiation from the different types of motion: cyclotron, z-bounce and magnetron. These states correspond to regular motion of the classical system. For weakly bound states, the cyclotron motion and z-bounce motion radiate faster than the magnetron motion. The magnetron motion has radiative lifetimes much longer than the lifetime in no magnetic field. Guest and Raithel [62] revisited this calculation, but for more deeply bound states the

motion is not as easily separable. They were able to identify the regions of adiabatic and diabatic motion as it appeared in their spectra with decreasing azimuthal quantum number.

The two previous studies showed that the radiative cascade is qualitatively changed for the most weakly bound states. Topçu and Robicheaux [63] examined the length of time that the $\bar{H}$ atoms took to radiate and reach the ground state as a function of principal quantum number and type of distribution in the azimuthal quantum number. They computed the radiative decay rates by diagonalizing the Hamiltonian in a basis and numerically computing the radiative decay rates to all lower energy states. The range examined here was exactly the region not treated in [61, 62], i.e. from medium principal quantum numbers down to the ground state. When the magnetic field is only strong enough to mix the states within a degenerate manifold, the cascade time is hardly changed from that with no magnetic field. At higher field strengths, there are some states that radiate much faster than for zero field and there are some that radiate much more slowly. The states that radiate faster are those that are attracted to a low magnetic field. For 4 T fields, the changes in the radiative decay start becoming strong for principal quantum numbers near 30.

Horbatsch *et al* [64] gave a treatment of the radiative decay when the magnetic field does not mix states of adjacent principal quantum number. They used a semiclassical method to obtain the radiative lifetimes. This method allows the calculation of the radiative lifetime without the need for the large basis set calculations of [63]. Also, it gives a different perspective on why various states radiate differently.

Wetzels *et al* [65] considered the possibility for driving states to lower principal quantum number using far infrared light. The peculiarity of this set-up was that the light that was to stimulate the downward transition could also ionize the atom. The interesting aspect of this paper was that it was possible to find a region of intensity and frequency where the downward transitions were much more likely than the ionization transitions, even in strong magnetic fields. The difficulty of applying these results to the $\bar{H}$ experiments is that the light is at an awkward wavelength and intensity.

Finally, we note that the radiative cascade could cause a spin flip due to the spin–orbit interaction. For example, if an electron is in the $m_\ell = \ell$ state with spin down, the spin–orbit interaction mixes it with the state with $m_\ell = \ell - 1$ with spin up. For no magnetic field, an atom that starts in an $n > 5, \ell = n - 1, m_\ell = \ell$ state with equal population of spin up and spin down has a population of 85% spin up when the ground state is reached. Thus, the magnetic moment from the orbital motion gets transferred to the spin magnetic moment. A strong magnetic field suppresses this effect due to the different magnetic moment of the orbital and spin degrees of freedom. For a 1 T field, an equal mixture of spin up and spin down evolves to a population of ∼70% spin up in the ground state. Thus, if the atoms are initially drawn from a population attracted to low fields through their orbital angular momentum, there will be an increase in the population attracted to low fields when they reach the ground state.

5. Different trapping scenarios

There have been a few different suggestions for mechanisms to trap the $\bar{H}$. The standard geometry appears to be one where mirror coils and a higher order multipole give a magnetic minimum. For this situation, the atom is trapped using the magnetic moment of the ground state. The well depth is then approximately 2/3 K for each 1 T change in the magnetic field. Depths of at least 1/2 K seem to be achievable. The stability of the positron and $\bar{p}$ plasmas in this type of trap is not guaranteed. The multipole field adds a non-axisymmetric field which can lead to plasma instabilities. Clearly, the plasmas will be more stable when the size of this perturbation is smaller which has led to the use of high-order multipoles.

Ohkawa and Miller [66] examined the possibility for using the electric polarizability of the ground state to trap the atom. A time-average maximum of the squared electric field can be obtained from a standing wave microwave mode. Unfortunately, the polarizability of the ground state is incredibly small and well depths of 0.01 K for a field of 1 MV cm^{-1} are obtained. The effect of such strong fields on the plasmas and temperature of the trap will surely make this mechanism unacceptable.

Dubin [67] considered three different designs for a magnetic trap. The first was a cylindrically symmetric trap which reduces the effect of plasma instabilities due to loss of symmetry. The trap design had a good potential well depth of 1 K, but it required a wire running through the centre of the trap. The second design used the idea of a time-averaged orbiting potential (TOP) trap where the magnetic field rotates around the axis. This design is cylindrically symmetric but only in the time-averaged sense. However, it is possible that the rotation could be designed to enhance the stability of the plasmas by providing a rotating wall effect. Unfortunately, the estimated well depth was of order 0.1 K. The last design was similar to the previous design but also used a high-order multipole to provide radial confinement.

Ordonez *et al* [68] reviewed some of the older proposals for producing magnetic fields for trapping neutrals and plasmas. Unfortunately, the only geometry that seemed to be both experimentally achievable and able to provide the plasma stability and well depth needed for $\bar{H}$ trapping was the standard geometry discussed in the first paragraph of this section. Nevertheless, [68] is a good presentation of the issues required for understanding the possibilities of different geometries.

Mohri and Yamazaki [69] proposed a completely different type of trap where the positrons are trapped by a combination of a magnetic quadrupole field with a superimposed electric octupole field. The octupole electric field is constructed so that the force along the magnetic field lines pushes the positrons back to the centre of the trap. The authors propose that beams of $\bar{H}$ can be obtained from this geometry. The plasma stability for this geometry has not been investigated.

6. Full simulation

There has only been one investigation that attempted to put together all of the above pieces and simulate the results of

[9, 10]. Robicheaux [70] reported the results of simulations that included all of the experimental properties without any adjustable parameters. In these experiments, the $\bar{p}$'s are launched through a positron plasma with at least a few electron volts of excess energy. They slow through the interaction with plasma waves and collisions with individual positrons. Once they are slow enough $\bar{H}$ formation can take place.

This simulation took into account the actual radius, length and voltage of each electrode, and the number of positrons and their density; the shape of the positron plasma is then determined by the requirement of thermal equilibrium and was calculated using a self-consistent algorithm for a grid of points in the trap. The motion of the $\bar{p}$ through the trap was computed by solving the classical equations of motion using the self-consistent fields from the positrons and the electrodes and the uniform magnetic field. The energy lost to plasma waves was calculated using the treatment of [18]. The recombination was taken to be purely from three-body recombination. The three-body recombination was calculated by firing positrons at the $\bar{p}$ while it was inside the positron plasma. The motion of the $\bar{H}$ was again calculated using the self-consistent fields. Whether the $\bar{H}$ could survive to reach the walls of the trap were found by simply following the motion and determining whether it reached the wall before being stripped by the electric fields in the trap.

The simulation found the number of $\bar{H}$ that should have been detected in each experiment. In both cases, the results of the simulations were in decent agreement with the experiments. Another important result of the simulation was the prediction that most of the $\bar{H}$ would be formed before the $\bar{p}$'s reached thermal equilibrium with the positron plasma. This result was found in both experiments [27, 71].

Robicheaux [70] emphasized two important consequences of the fact that the three-body recombination is started and then quickly stopped. The binding energy of the $\bar{H}$'s tend to be less than expected. This is because there is no time for many positron collisions with the $\bar{H}$'s to drive them to lower energy. Second, the temperature dependence of the number of $\bar{H}$'s does not need to be related to the steady state temperature dependence. This is because the experiments are measuring a branching ratio: the fraction of $\bar{H}$'s that form and can reach the detection region compared to the number of $\bar{p}$'s involved in a process that takes them out of contact with the positron plasma. The simulations found that the number of recombined $\bar{H}$'s did not decrease nearly as fast as $T^{-9/2}$. Amoretti *et al* [72] found that the number of $\bar{H}$'s decreased roughly as T^{-1} but over a much larger energy range than that checked in [70].

7. Concluding thoughts

This review has attempted to treat all of the atomic processes that are important for understanding the results of recent experiments on $\bar{H}$. There are only two areas that have been deliberately avoided since they both relate to using $\bar{H}$ and are topics well outside my areas of expertise. The first and most important area is the physics of high-resolution spectroscopy of the 1s–2s transition. A subset of this are the theoretical investigations into the most promising parameter ranges for external fields to see CPT violations and possible exotic physics [73]. The second area is the interaction of the $\bar{H}$ with neutral matter. Typically, this mainly focuses on the scattering and/or annihilation from simple atoms (e.g. H) or molecules (e.g. H_2).

In treating the processes covered in this review, I wanted to emphasize the features important for a qualitative understanding. I am hopeful that this will allow someone to estimate the level of importance of a given process and/or the possibility that a proposed scheme will work. But I also wanted to convey that while it is useful to understand these processes in order to make sense of the experiments, the behaviour of this relatively simple atomic system is inherently interesting and challenging.

Acknowledgments

This work was supported by the Chemical Sciences, Geosciences, and Biosciences Division of the Office of Basic Energy Sciences, U.S. Department of Energy and by the Office of Fusion Energy, U.S. Department of Energy.

References

[1] Gabrielse G 2005 *Adv. At. Mol. Phys.* **50** 155
[2] Gabrielse G *et al* 1988 *Phys. Lett.* A **129** 38
[3] Bertsche W *et al* (ALPHA Collaboration) 2006 *Nucl. Instrum. Methods Phys. Res.* A **566** 746
[4] Jorgensen L V *et al* (ALPHA Collaboration) 2008 *Nucl. Instrum. Methods* B **266** 357
[5] Gabrielse G *et al* (ATRAP Collaboration) 2008 *Phys. Rev. Lett.* **100** 113001
[6] Andresen G B *et al* (ALPHA Collaboration) 2008 *Phys. Rev. Lett.* **100** 203401
[7] Jackson J D 1999 *Classical Electrodynamics* (New York: Wiley) p 770
[8] O'Neil T M 1983 *Phys. Fluids* **26** 2128
[9] Amoretti M *et al* (ATHENA Collaboration) 2002 *Nature* **419** 456
[10] Gabrielse G *et al* (ATRAP Collaboration) 2002 *Phys. Rev. Lett.* **89** 213401
[11] O'Neil T M and Hjorth P G 1985 *Phys. Fluids* **28** 3241
[12] Hjorth P G and O'Neil T M 1987 *Phys. Fluids* **30** 2613
[13] Glinsky M E *et al* 1992 *Phys. Fluids* B **4** 1156
[14] Robicheaux F and Fajans J 2007 *J. Phys. B: At. Mol. Opt. Phys.* **40** 3143
[15] Amoretti M *et al* (ATHENA Collaboration) 2004 *Phys. Lett.* B **590** 133
[16] Kellerbauer A and Walz J 2006 *New J. Phys.* **8** 45
[17] Mollers B *et al* 2004 *Nucl. Instrum. Methods Phys. Res.* A **532** 279
[18] Nersisyan H B, Walter M and Zwicknagel G 2000 *Phys. Rev.* E **61** 7022
[19] Geller D K and Weisheit J C 1997 *Phys. Plasmas* **4** 4258
[20] Koryagin S A 2000 *JETP* **90** 741
[21] Toepffer C 2002 *Phys. Rev.* A **66** 022714
[22] Hurt J L *et al* 2008 *J. Phys. B: At. Mol. Opt. Phys.* **41** 165206
[23] Taylor C L, Zhang J J and Robicheaux F 2006 *J. Phys. B: At. Mol. Opt. Phys.* **39** 4945
[24] Pohl T *et al* 2006 *Phys. Rev. Lett.* **97** 213001
[25] Cesar C L, Zagury N and Robicheaux F 2008 *J. Phys. B: At. Mol. Opt. Phys.* submitted
[26] Gabrielse G *et al* (ATRAP Collaboration) 2002 *Phys. Rev. Lett.* **89** 233401

[27] Gabrielse G *et al* (ATRAP Collaboration) 2004 *Phys. Rev. Lett.* **93** 073401
[28] Pohl T, Sadeghpour H R and Gabrielse G 2006 *Phys. Rev. Lett.* **97** 143401
[29] Fano U, Robicheaux F and Rau A R P 1988 *Phys. Rev.* A **37** 3655
[30] Choi J-H *et al* 2005 *Phys. Rev. Lett.* **95** 243001
[31] Kuzman S G, O'Neil T M and Glinsky M E 2004 *Phys. Plasmas* **11** 2382
[32] Vrinceanu D *et al* 2004 *Phys. Rev. Lett.* **92** 133402
[33] Carter B P 1969 *J. Math. Phys., NY* **10** 788
[34] Kuzmin S G and O'Neil T M 2004 *Phys. Rev. Lett.* **92** 243401
[35] Kuzmin S G and O'Neil T M 2005 *Phys. Plasmas* **12** 012101
[36] Dubin D H E 2004 *Phys. Rev. Lett.* **92** 195002
[37] Hu S X *et al* 2005 *Phys. Rev. Lett.* **95** 163402
[38] Vrinceanu D *et al* 2005 *Phys. Rev.* A **72** 042503
[39] Garton W R S and Tomkins F S 1969 *Astrophys. J.* **158** 839
[40] Horndl M *et al* 2003 *Hyp. Int.* **146** 13
[41] Correa C E, Correa J R and Ordonez C A 2005 *Phys. Rev.* E **72** 046406
[42] Yousif F B *et al* 1991 *Phys. Rev. Lett.* **67** 26
[43] Rogelstad M L *et al* 1997 *J. Phys. B: At. Mol. Opt. Phys.* **30** 3913
[44] Amoretti M *et al* (ATHENA Collaboration) 2006 *Phys. Rev. Lett.* **97** 213401
[45] Scrinzi A, Elander N and Wolf A 1995 *Z. Phys.* D **34** 185
[46] Wesdorp C, Robicheaux F and Noordam L D 2000 *Phys. Rev. Lett.* **84** 3799
Wesdorp C, Robicheaux F and Noordam L D 2001 *Phys. Rev.* A **64** 033414
[47] Hessels E A, Homan D M and Cavagnero M J 1998 *Phys. Rev.* A **57** 1668
[48] Storry C H *et al* 2004 *Phys. Rev. Lett.* **93** 263401
[49] Speck A *et al* 2004 *Phys. Lett.* B **597** 257
[50] Wall M L, Norton C S and Robicheaux F 2005 *Phys. Rev.* A **72** 052702
[51] Lu J, Sidky E Y, Roller-Lutz Z and Lutz H O 2003 *Phys. Rev.* A **68** 024702
[52] Chattopadhyay A and Sinha C 2006 *Phys. Rev.* A **74** 022501
[53] Glinsky M E and O'Neil T M 1991 *Phys. Fluids* B **3** 1279
[54] Driscoll C F 2004 *Phys. Rev. Lett.* **92** 149303
[55] Gabrielse G *et al* (ATRAP Collaboration) 2004 *Phys. Rev. Lett.* **92** 149304
[56] Robicheaux F and Hanson J D 2004 *Phys. Rev.* A **69** 010701(R)
[57] Robicheaux F 2006 *Phys. Rev.* A **73** 033401
[58] Robicheaux F 2007 *J. Phys. B: At. Mol. Opt. Phys.* **40** 271
[59] Fedichev P O 1997 *Phys. Lett.* A **226** 289
[60] Bass E M and Dubin D H E 2004 *Phys. Plasmas* **11** 1240
[61] Guest J R, Choi J-H and Raithel G 2003 *Phys. Rev.* A **68** 022509
[62] Guest J R and Raithel G 2003 *Phys. Rev.* A **68** 052502
[63] Topçu T and Robicheaux F 2005 *Phys. Rev.* A **73** 043405
[64] Horbatsch M W, Hessels E A and Horbatsch M 2005 *Phys. Rev.* A **72** 033405
[65] Wetzels A *et al* 2006 *Phys. Rev.* A **73** 062507
[66] Ohkawa T and Miller R L 2004 *Phys. Plasmas* **11** 1730
[67] Dubin D H E 2001 *Phys. Plasmas* **8** 4331
[68] Ordonez C A *et al* 2002 *Phys. Plasmas* **9** 3289
[69] Mohri A and Yamazaki Y 2003 *Europhys. Lett.* **63** 207
[70] Robicheaux F 2004 *Phys. Rev.* A **70** 022510
[71] Madsen N *et al* (ATHENA Collaboration) 2005 *Phys. Rev. Lett.* **94** 033403
[72] Amoretti M *et al* (ATHENA Collaboration) 2004 *Phys. Lett.* B **583** 59
[73] Kellerbauer A *et al* (AEGIS Proto-Collaboration) 2008 *Nucl. Instrum. Methods* B **266** 351